



## Adsorption and corrosion inhibition of new synthesized Pyridazinium-Based Ionic Liquid on Carbon steel in 0.5 M H<sub>2</sub>SO<sub>4</sub>

L. Messaadia<sup>1,2</sup>, O. ID El mouden<sup>2</sup>, A. Anejjar<sup>2</sup>, M. Messali<sup>3</sup>, R. Salghi<sup>2,\*</sup>,  
O. Benali<sup>4</sup>, O. Cherkaoui<sup>5</sup>, A. Lallam<sup>6</sup>

<sup>1</sup>Université de Mohamed Seddik Ben Yahia, Faculté des Sciences Exactes et Informatique, Département de Chimie, B.P. 98 Ouled AïSSA Jijel, 18000 Algérie

<sup>2</sup>Laboratory of Environmental Engineering and Biotechnology, ENSA, Ibn Zohr University, PO Box 1136, 80000 Agadir, Morocco

<sup>3</sup>Chemistry of Department, Faculty of Science, Taibah University, 30002, Al-Madinah Al-Mounawwara, Saudi Arabia

<sup>4</sup>Department of Biology, Faculty of sciences, Dr. Tahar Moulay University of Saïda- Algeria

<sup>5</sup>Research and Development Laboratory, Ecole Supérieure des Industries du Textiles et de l'Habillement, Casablanca, Morocco

<sup>6</sup>Laboratoire de Physique and Mécanique Textile, EAC 7189, UHA, Mulhouse, France

Received 1 Sept 2014, Revised 1 Dec 2014, Accepted 2 Dec 2014

\*Corresponding author: E-mail: [r.salghi@uiz.ac.ma](mailto:r.salghi@uiz.ac.ma)

### Abstract

The corrosion inhibition properties of 1-(2-ethoxy-2-oxoethyl) pyridazinium chloride (EOPC) on carbon steel (CS) in sulfuric acid (0.5 M H<sub>2</sub>SO<sub>4</sub>) solution has been examined and characterized by weight loss, potentiodynamic polarization and electrochemical impedance spectroscopy (EIS) measurements. The experimental results reveal that the compound has a good inhibiting effect on the metal tested in 0.5M H<sub>2</sub>SO<sub>4</sub> solution. The inhibition efficiency for this compound studied increased with the increase in the inhibitor concentrations to attain 91.67 % at the 10<sup>-3</sup> M of EOPC. Polarization curves showed that EOPC acted as a mixed-type inhibitor in sulfuric acid. EIS results show that the change in the impedance parameters (R<sub>i</sub> and C<sub>dl</sub>) with concentration of EOPC is indicative of the adsorption of molecules leading to the formation of a protective layer on the surface of carbon steel. The effect of the temperature on the corrosion behavior with addition of 10<sup>-3</sup>M of the inhibitor was studied in the temperature range 298-328 K, and the thermodynamic parameters were determined and discussed. The adsorption of this compound on CS surface obeys Langmuir's adsorption isotherm.

**Keywords:** Carbon steel ; EIS ; Polarisation ; Pyridazinium ; Adsorption.

### 1. Introduction

Corrosion is one of the major problems in several technical installations involving metals and alloys today hence, prevention mechanism for corrosion of metals is of paramount important to increase their lifespan especially those in aggressive environments. The corrosion of metallic materials in acidic solution causes considerable loss. In order to reduce the corrosion of metals several techniques have been adopted. The use of corrosion inhibitors constitutes one of the most economical ways to mitigate the corrosion rate, preserve industrial facilities and protect metal surfaces against corrosion in acidic media [1-10]. Acid solutions are commonly used for removal of undesirable scale and rust in metal finishing industries, cleaning of boilers and heat exchangers. Sulfuric acid is generally the superior choice over the other mineral acids for steel surface treatment basically due to its lower cost, minimal fumes and non-corrosive nature of the SO<sub>4</sub><sup>2-</sup> ion [11-12]. The development of corrosion inhibitors is based on organic compounds containing nitrogen, oxygen, sulphur atoms, and multiple bonds in the molecules that facilitate adsorption on the metal surface [13-21]. In general, the adsorption of an inhibitor on a metal surface depends on the nature and the surface charge of the metal, the adsorption mode, its chemical structure and the type of electrolyte solution [22-28]. The inhibition efficiency should increase in the order O<N<S<P [26]. In our laboratory, many studies have been published on the use of natural products as corrosion inhibitors in acidic media [29-40], but little work appears to have been done on the corrosion inhibition of steel alloys in sulphuric acid using pyridazinium derivatives. The aim of the present study was to examine the inhibitive action of a new pyridazinium-based ionic liquid compound, namely 1-(2-

ethoxy-2-oxoethyl) pyridazinium chloride (**EOPC**) on the behavior of carbon steel corrosion in 0.5 M sulfuric acid solution. The chemical structures of the studied pyridazinum ionic liquids are given in Figure 1.

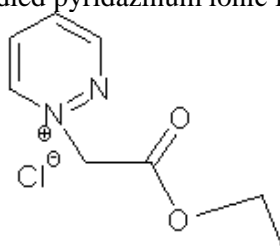


**Figure 1:** The chemical structure of **EOPC**

## 2. Materials and methods

### 2.1. Material preparation and solutions

The steel used in this study is a carbon steel (Euronorm: C35E carbon steel and US specification: SAE 1035) with a chemical composition (in wt%) of 0.370 % C, 0.230 % Si, 0.680 % Mn, 0.016 % S, 0.077 % Cr, 0.011 % Ti, 0.059 % Ni, 0.009 % Co, 0.160 % Cu and the remainder iron (Fe). The aggressive solution 0.5 M sulfuric acid was prepared by dilution of an Analytical Grade 98% H<sub>2</sub>SO<sub>4</sub> with double distilled water. All experiments were carried out in 0.5 M H<sub>2</sub>SO<sub>4</sub> solution in the absence and presence of different concentrations of **EOPC**.

### 2.2. Gravimetric analysis

Gravimetric measurements were carried out in a double walled glass cell equipped with a thermostat cooling condenser. The CS specimens used have a rectangular form (2 × 2 × 0.08 cm<sup>3</sup>). The duration of tests was 6 h at 298 K in 0.5 M H<sub>2</sub>SO<sub>4</sub> solution containing different concentrations of **EOPC**. The specimens were abraded with a series of emery paper (grade 800–1200) and then washed thoroughly with ethanol and double distilled water. After weighing precisely, the specimens were immersed in beakers which contained 80 ml acid solutions with different concentrations of **EOPC** at a certain temperature maintained by a water thermostat. All the aggressive acid solutions were open to air. After 6 h the specimens were taken out, washed, dried, and weighed exactly.

### 2.3. Electrochemical measurements

#### 2.3.1. Potentiodynamic polarization

The electrochemical measurements were carried out using Volta lab (PGZ 100) potentiostat and controlled by software model (Voltmaster 4) at under static condition. The corrosion cell used had three electrodes. The reference electrode was a saturated calomel electrode (SCE). A platinum electrode was used as auxiliary electrode. The working electrode was carbon steel (CS). All potentials given in this study were referred to this reference electrode. The working electrode was immersed in test solution for 30 minutes to establish steady state open circuit potential (E<sub>ocp</sub>). After measuring the E<sub>ocp</sub>, the electrochemical measurements were performed. All electrochemical tests have been performed in aerated solutions at 298 K. The electrochemical behaviour of CS sample in inhibited and uninhibited solution was studied by recording anodic and cathodic potentiodynamic polarization curves. Measurements were performed in the 0.5M H<sub>2</sub>SO<sub>4</sub> solution containing different concentrations of the tested inhibitor by changing the electrode potential automatically from -800 mV to -200 mV versus corrosion potential at a scan rate of 1 mV. s<sup>-1</sup>. The linear Tafel segments of anodic and cathodic curves were extrapolated to corrosion potential to obtain corrosion current densities (I<sub>corr</sub>).

#### 2.3.2. Electrochemical impedance spectroscopy (EIS)

The EIS experiments were conducted in the frequency range with high limit of 100 kHz and different low limit 0.1 Hz at open circuit potential, with 10 points per decade, at the rest potential, after 30 min of acid immersion, by applying 10 mV ac voltage peak-to-peak. Nyquist plots were made from these experiments. The best semicircle can be fit through the data points in the Nyquist plot using a non-linear least square fit so as to give the intersections with the x-axis.

## 3. Results and discussion

### 3.1. Weight loss tests

The corrosion rate (W<sub>corr</sub>) of tested metal in 0.5 M H<sub>2</sub>SO<sub>4</sub> solution at different concentrations of **EOPC** was determined after 6 h of immersion time at 298 K. The obtained values of the gravimetric corrosion rates (W<sub>corr</sub>) and the inhibition efficiency (E<sub>w</sub> %) are represented in Table 1. The inhibition efficiency corrosion in the case of this method was calculated from the following equation:

$$E_w (\%) = \frac{W_{\text{corr}} - W'_{\text{corr}}}{W_{\text{corr}}} \times 100 \quad (1)$$

where  $W_{\text{corr}}$  and  $W'_{\text{corr}}$  are the corrosion rate of CS in 0.5 M  $\text{H}_2\text{SO}_4$  in absence and presence of inhibitor, respectively.

**Table 1.** Effect of **EOPC** concentration on corrosion data of CS in 0.5 M  $\text{H}_2\text{SO}_4$ .

Conc (M)	$W_{\text{corr}}$ (mg. $\text{cm}^{-2}$ )	$E_w$ (%)
Blank	1.011	----
$10^{-3}$	0.091	<b>90.99</b>
$10^{-4}$	0.154	<b>84.77</b>
$10^{-5}$	0.212	<b>79.03</b>
$10^{-6}$	0.301	<b>70.23</b>

Results obtained from gravimetric measurements show for inhibitor tested that the corrosion rate values decrease when the concentration of **EOPC** increases. The analysis of Table 1 show that protection efficiency increased with increasing concentration of inhibitor studied. We noted that **EOPC** used in this study showed very excellent corrosion inhibitor for CS in 0.5 M  $\text{H}_2\text{SO}_4$ , especially for low concentration (70.23 % for  $10^{-6}$ ). The best action is attained in the presence of  $10^{-3}$ M of **EOPC**.

### 3.2. Polarization results

The potentiodynamic polarization curves of CS performed in 0.5 M  $\text{H}_2\text{SO}_4$  in the absence and the presence of different concentrations of **EOPC** at 298 K are presented in Figure 2. The values of electrochemical parameters associated with polarization measurements, such as corrosion potential ( $E_{\text{corr}}$ ), corrosion currents densities ( $I_{\text{corr}}$ ) and cathodic Tafel slope ( $\beta_c$ ) are listed in Table 2.

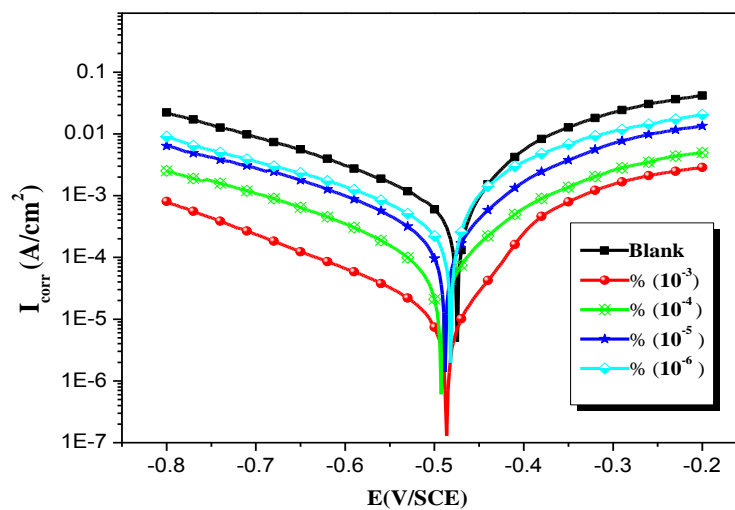


**Figure 2.** Potentiodynamic polarisation curves of CS in 0.5 M  $\text{H}_2\text{SO}_4$  in the presence of different concentrations of **EOPC**.

The inhibition efficiency  $E_I$  (%) is calculated from the values of  $I_{\text{corr}}$  with the relation:

$$E_I(\%) = \frac{I_{\text{corr}} - I'_{\text{corr}}}{I_{\text{corr}}} \times 100 \quad (2)$$

Where  $I_{\text{corr}}$  and  $I'_{\text{corr}}$  are uninhibited and inhibited corrosion current densities, respectively.

It is clear from the Figure 2, that both anodic metal dissolution and cathodic hydrogen reduction reactions were inhibited when the **EOPC** inhibitor was added to 0.5 M  $\text{H}_2\text{SO}_4$ . The corrosion potential is almost unchanged. The corrosion current density as well as corrosion rate of CS considerably reduced in the presence of the inhibitor.

**Table 2.** Electrochemical parameters of CS at various concentrations of **EOPC** in 0.5 M H<sub>2</sub>SO<sub>4</sub> and corresponding inhibition efficiency.

Conc. (M)	-E <sub>corr</sub> (mV/SCE)	I <sub>corr</sub> (μA/cm <sup>2</sup> )	-b <sub>c</sub> (mV/dec)	E <sub>i</sub> (%)
Blank	478	1860	190	----
10 <sup>-3</sup>	486	163	188	<b>91.24</b>
10 <sup>-4</sup>	492	258	215	<b>86.13</b>
10 <sup>-5</sup>	489	367	185	<b>80.27</b>
10 <sup>-6</sup>	481	491	204	<b>73.60</b>

The results are indicative of the adsorption of inhibitor molecules on the CS surface. The inhibition of both anodic and cathodic reactions is more marked with the increasing inhibitor concentration while the corrosion potential nearly remained the same in comparison with corrosion potential observed in blank solution. These results indicate that the **EOPC** is a mixed-type inhibitor for the corrosion of CS in 0.5 M H<sub>2</sub>SO<sub>4</sub> [41]. The inspection of results in Table 2 indicate that **EOPC** inhibits the corrosion process in the studied range of concentrations and E<sub>i</sub> (%) increases with these later, reaching its maximum value, 91.24%, at 10<sup>-3</sup> M.

### 3.3. Electrochemical impedance spectroscopy measurements

The corrosion behavior of CS in 0.5 M H<sub>2</sub>SO<sub>4</sub> solution in the absence and presence of different concentrations of **EOPC** was investigated by the EIS method at 298K after 30 min of immersion. Fig. 3 shows the Nyquist plot for CS in 0.5 M H<sub>2</sub>SO<sub>4</sub> solution in the absence and presence of different concentrations of investigated inhibitor.

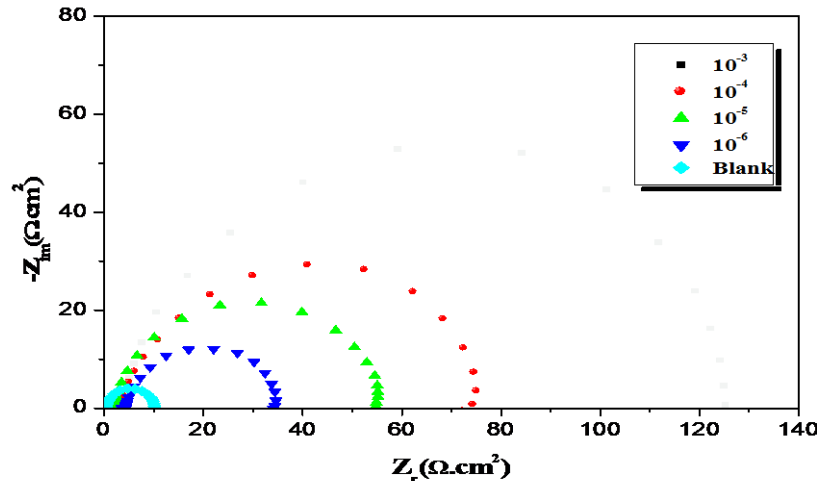


**Figure 3.** Nyquist plots of CS in 0.5 M H<sub>2</sub>SO<sub>4</sub> without and with different concentration of **EOPC** at 298K.

The charge-transfer resistance values (R<sub>ct</sub>) were calculated from the difference in impedance at lower and higher frequencies as suggested by Tsuru et al. [42]. The double-layer capacitance (C<sub>dl</sub>) and the frequency at which the imaginary component of the impedance is maximal (-Z''<sub>max</sub>) are found as represented in equation:

$$C_{dl} = \left( \frac{1}{w \cdot R_{ct}} \right) \quad \text{where} \quad w = 2 \cdot \pi \cdot f_{max} \quad (3)$$

with C<sub>dl</sub>: Double layer capacitance (μF.cm<sup>-2</sup>); f<sub>max</sub>: maximum frequency (Hz) and R<sub>ct</sub>: Charge transfer resistance (Ω.Cm<sup>-2</sup>).

The inhibition efficiency got from the charge transfer resistance is calculated by:

$$E_R(\%) = \frac{R_{ct} - R_{ct}^0}{R_{ct}} \times 100 \quad (4)$$

where  $R_{ct}$  and  $R_{ct}^0$  are the charge transfer resistances in inhibited and uninhibited solutions respectively.

The values of charge transfer resistance  $R_{ct}$ , double layer capacitance  $C_{dl}$  and inhibition efficiency  $E_R$ , for the corrosion of CS in 0.5 M  $H_2SO_4$  with different concentration of inhibitors are listed in Table 2. The presence of inhibitors concentration enhance the values of  $R_{ct}$  and reduces the  $C_{dl}$  may be due to the adsorption of inhibitors to form an adherent film on the metal surface and suggests that the coverage of the metal surface with this film increases the double layer thickness [43]. The value of the inhibition efficiency  $E_R(\%)$  for the corrosion of CS in 0.5 M  $H_2SO_4$  increase with increasing of the inhibitor concentration.

These EIS measurements were in good agreement with the corrosion weight loss and polarization curves.

**Table 2** Electrochemical Impedance parameters for corrosion of steel in acid medium at various concentration of Pyridazinium.

Conc. (M)	$R_t (\Omega \cdot cm^2)$	$C_{dl} (\mu F \cdot cm^{-2})$	$E_R (\%)$
Blank	10	221.16	----
$10^{-3}$	125	31.85	<b>91.67</b>
$10^{-4}$	74	28.69	<b>86.49</b>
$10^{-5}$	54	29.49	<b>81.48</b>
$10^{-6}$	34	31.22	<b>70.58</b>

### 3.4. Effect of temperature

Temperature can modify the interaction between the CS electrode and the acidic medium in the absence and the presence of inhibitors. To assess the influence of temperature on corrosion and corrosion inhibition processes, polarization tests were carried out at various temperatures (298–328 K) in the absence and presence of  $10^{-3}$  M of **EOPC**, as shown in Figures 4 and 5.

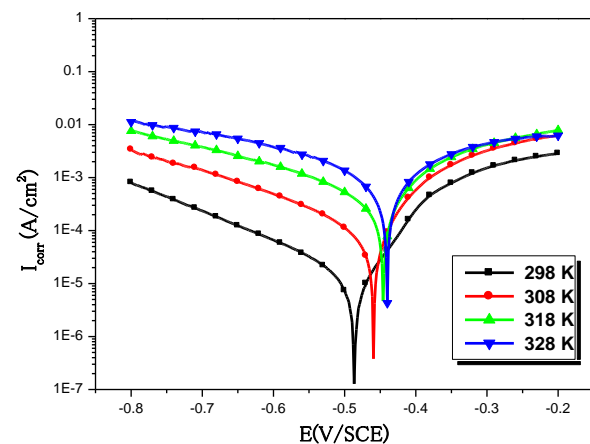
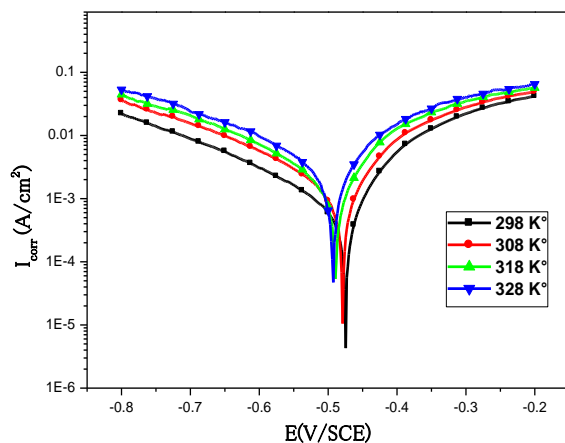


**Figure 4.** Polarisation curves of CS in 0.5 M  $H_2SO_4$  at different temperature.

**Figure 5.** Polarisation curves of CS in 0.5 M  $H_2SO_4$  in the presence of  $10^{-3}$  M of **EOPC** at different temperatures

Electrochemical parameters such as corrosion current density ( $I_{corr}$ ), corrosion potential ( $E_{corr}$ ), cathodic Tafel slope ( $\beta_c$ ), and the inhibition efficiency ( $E_I \%$ ) were determined by Tafel extrapolation method and are given in Table 3. These values were calculated from the intersection of the anodic and cathodic Tafel lines of the polarisation curve at  $E_{corr}$ .

Examination of Table 3 revealed that an increase in temperature increases  $I_{corr}$ , while the addition of **EOPC** decreases the  $I_{corr}$  values across the temperature range. The results also indicate that the inhibition efficiencies

decreased proportionally with temperature. This can be explained by the decrease of the strength of adsorption processes at elevated temperature and suggested a physical adsorption mode.

**Table 3.** Effect of temperature on the steel corrosion in the absence and presence of **EOPC** at different concentrations.

	Temp. (K)	E <sub>corr</sub> (mV/SCE)	I <sub>corr</sub> (μA/cm <sup>2</sup> )	β <sub>c</sub> (mV/dec)	E <sub>I</sub> (%)
<b>Blank</b>	298	-478	1860	-190	----
	308	-483	2754	-151	----
	318	-493	3036	-126	----
	328	-497	4511	-104	----
<b>EOPC</b>	298	486	163	188	<b>91.23</b>
	308	-460	281	218	<b>89.79</b>
	318	-446	582	276	<b>80.83</b>
	328	-441	1385	283	<b>69.29</b>

The values of activation energy E<sub>a</sub>, activation enthalpy ΔH<sub>a</sub> and activation entropy were estimated using Arrhenius equation and transition state equation) [29, 40]:

$$I_{\text{corr}} = A \exp\left(\frac{-E_a}{RT}\right) \quad (5)$$

$$I_{\text{corr}} = \frac{RT}{Nh} \exp\left(\frac{\Delta S_a}{R}\right) \exp\left(\frac{-\Delta H_a}{RT}\right) \quad (6)$$

Where A is the Arrhenius factor, R is the perfect gas constant, N is Avogadro's number, h is Plank's constant, ΔS<sub>a</sub> and ΔH<sub>a</sub> the entropy and enthalpy of activation, respectively.

Plots of ln(I<sub>corr</sub>) vs. 1000/T and ln(I<sub>corr</sub>/T) vs. 1000/T gave straight lines with slopes of (-E<sub>a</sub>/R) and (-ΔH<sub>a</sub>/R), respectively. The intercepts were A and (ln R/Nh + ΔS<sub>a</sub>/R) for the Arrhenius and transition state equations, respectively. Figs. 6 and 7 represent the data plots of ln(I<sub>corr</sub>) vs. 1000/T and ln(I<sub>corr</sub>/T) vs. 1000/T in the absence and presence of 10<sup>-3</sup>M of **EOPC**.

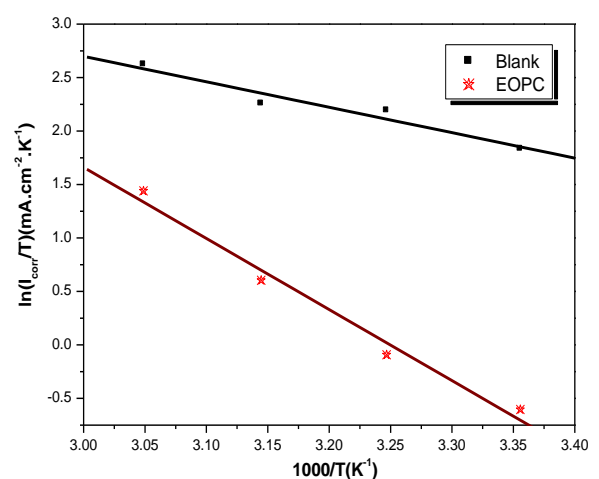
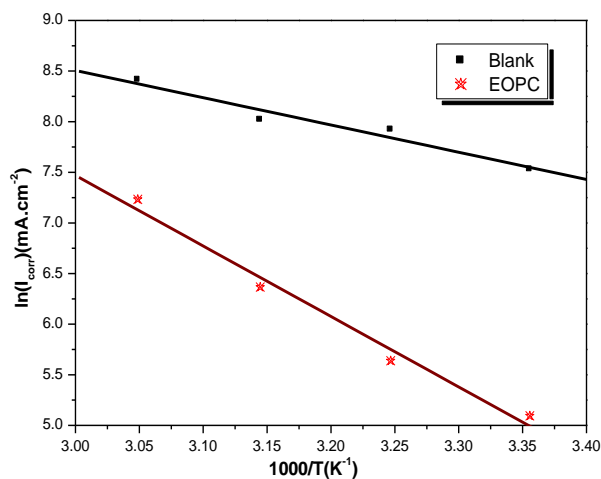


**Figure 6.** Arrhenius plots of steel in 0.5 M H<sub>2</sub>SO<sub>4</sub> with and without 10<sup>-3</sup>M of **EOPC**

**Figure 7.** Relation between ln(I<sub>corr</sub>/T) and 1000/T in acid at different temperatures.

The calculated values of E<sub>a</sub>, ΔH<sub>a</sub> and ΔS<sub>a</sub> are tabulated in Table 4. The data listed in this Table show that value of E<sub>a</sub> found for **EOPC** is higher than that obtained for 0.5 M H<sub>2</sub>SO<sub>4</sub> solution and consequently the rate of corrosion decreases.

**Table 4.** The values of activation parameters for CS in 0.5 M H<sub>2</sub>SO<sub>4</sub> in the absence and the presence of 10<sup>-3</sup> M of EOPC.

	Conc. (M)	E <sub>a</sub> (kJ/mol)	ΔH <sub>a</sub> (kJ/mol)	ΔS <sub>a</sub> (J/mol. K)	E <sub>a</sub> -ΔH <sub>a</sub> (KJ/mol)
Blank	0	22.37	19.77	-115.71	2.60
EOPC	10 <sup>-3</sup>	57.85	55.25	-17.89	2.60

The increase in the apparent activation energy may be interpreted on the basis of physical adsorption occurring in the first stage [44]. On the other hand, the positive sign of ΔH<sub>a</sub> shows that the corrosion process of CS is an endothermic phenomenon signifying that its dissolution is slow in the presence of EOPC [45]. On comparing the values of the entropy of activation ΔS<sub>a</sub> given in Table 6, it is clear that entropy of activation decreases more negatively in the presence of EOPC than in the absence of inhibitor; this reflects the formation of an ordered stable layer of inhibitor on the CS surface [46].

### 3.5. Adsorption isotherm

The mechanism of the interaction between inhibitor and the electrode surface can be explained using adsorption isotherms. Several adsorption isotherms were tested and the Langmuir adsorption isotherm was found to provide best description of the adsorption behavior of the investigated inhibitor. The Langmuir isotherm is given by the equation [47]:

$$\frac{C_{inh}}{\theta} = \frac{1}{K} + C_{inh} \quad (7)$$

$$\text{with } K = \frac{1}{55.5} \exp\left(\frac{-\Delta G_{ads}}{RT}\right)$$

Where C<sub>inh</sub> is the concentration of inhibitor, K the adsorptive equilibrium constant, ΔG<sub>ads</sub> is the standard free energy of adsorption reaction, R is the universal gas constant, T is the absolute temperature in Kelvin, θ is the fraction of the surface covered calculated as follows

θ = E<sub>w</sub>(%)/100 and the value of 55.5 is the concentration of water in the solution in mol/L. Fig. 8 shows the dependence of the ratio C<sub>inh</sub>/θ as function of C<sub>inh</sub>. Linear plot is obtained with slope and correlation coefficient close to 1.

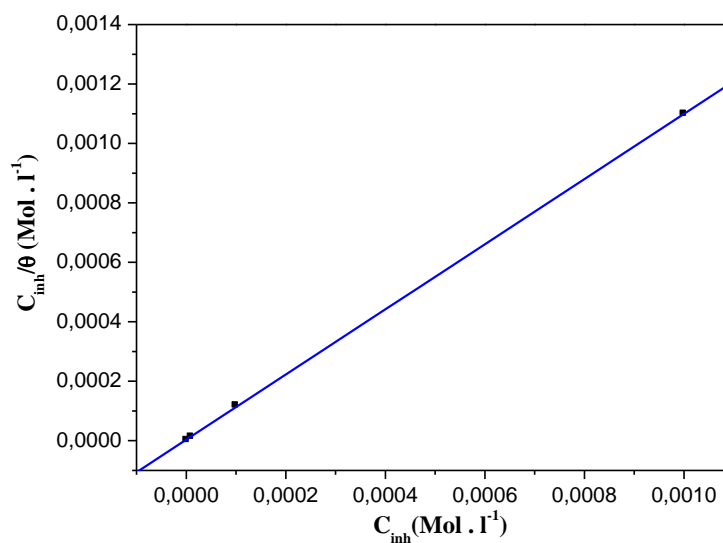


**Figure 8.** Langmuir adsorption plot of CS in 0.5 M H<sub>2</sub>SO<sub>4</sub> solution containing various concentrations of EOPC.

The equilibrium adsorption constant obtained from this isotherm are about  $3 \times 10^5 \text{ M}^{-1}$ . This is in good agreement with values of inhibition efficiency obtained from the electrochemical and weight loss measurements. Moreover, the largest negative values of  $\Delta G_{\text{ads}} = -41.20 \text{ kJ/mol}$  indicate that this inhibitor is strongly and spontaneous adsorbed onto the mild steel surface. We can note that a plausible mechanism of corrosion inhibition of carbon steel in 0.5 M  $\text{H}_2\text{SO}_4$  by the compound under study may be deduced on the basis of adsorption. In acidic solutions, this inhibitor exist as cationic species which may be adsorbed on the cathodic sites of the mild steel and reduce the evolution of hydrogen [15]. The protonated inhibitor can also be adsorbed on the metal surface on specifically adsorbed chloride ions [48-49], which act as a bridge between the metal surface and the electrolyte. Moreover, the adsorption of this compound on anodic sites through lone pairs of electrons of nitrogen and oxygen atoms and through  $\pi$ -electrons of  $\text{C}=\text{O}$  and pyridazinium group will then reduce the anodic dissolution of carbon steel. Generally, the standard free energy values of  $-20 \text{ kJ mol}^{-1}$  or less negative are associated with an electrostatic interaction between charged molecules and charged metal surface (physical adsorption); those of  $-40 \text{ kJ mol}^{-1}$  or more negative involves charge sharing or transfer from the inhibitor molecules to the metal surface to form a co-ordinate covalent bond (chemical adsorption) [50]. The calculated standard free energy of adsorption value is closer to  $-40 \text{ kJ mol}^{-1}$ . Therefore, it can be concluded that the adsorption is more chemical than physical adsorption [51].

## Conclusion

From the principal result of the present work we can conclude that:

- The pyridazinium derivative (**EOPC**) was found to perform in 0.5 M  $\text{H}_2\text{SO}_4$ .
- Polarization study showed that the compound under investigation was mixed type inhibitor.
- The inhibition efficiency of the **EOPC** increased with the concentration and reached **91.67 %** at  $10^{-3} \text{ M}$ .
- The weight loss, polarization curves and electrochemical impedance spectroscopy were in good agreement.
- The inhibition efficiency decreased with increasing temperature and their addition led to a increase of the activation corrosion energy.
- Adsorption of the inhibitor on the carbon steel surface from 0.5 M  $\text{H}_2\text{SO}_4$  followed the Langmuir isotherm.

## Reference

1. Sastri V. S., *Green Corrosion Inhibitors. Theory and Practice*, John Wiley & Sons: Hoboken, NJ; 1998.
2. Ouici H.B., Benali O., Harek Y., Larabi L., Hammouti B., Guendouzi A., *Res. Chem. Intermed. doi 10.1007/s11164-012-0797-1*(2015).
3. Bammou L., Chebli B., Salghi R., Bazzi L., Hammouti B., Mihit M., El Idrissi H., *Green Chem. Lett. Rev.* 3 (2010) 173.
4. Yüce A. O., Kardas G., *Corros. Sci.* 58 (2012) 86.
5. Zarrok H., Oudda H., Zarrouk A., Salghi R., Hammouti B., Bouachrine M., *Der Pharm. Chem.* 3 (2011) 576.
6. Bammou L., Mihit M., Salghi R., Bazzi L., Bouyanzer A., Hammouti B., *Int. J. Electrochem. Sci.* 2011, 6, 1454.
7. Ben Hmamou D., Salghi R., Zarrouk A., Hammouti B., Al-Deyab S. S., Bazzi Lh., Zarrok H., Chakir A., Bammou L., *Int. J. Electrochem. Sci.* 7(2012) 2361.
8. Afia L., Salghi R., Bammou L., Bazzi Lh., Hammouti B., Bazzi L., *Acta Metall. Sin.* 25 (2012)10.
9. Afia L., Salghi R., Zarrouk A., Zarrok H., Benali O., Hammouti B., Al-Deyab S.S., Chakir A., Bazzi L., *Port. Electrochim. Acta.* 30 (4) (2012) 267
10. Afia L., Salghi R., Zarrouk A., Zarrok H., Bazzi Lh., Hammouti B., Zougagh M., *Trans Indian Inst. Met.* 66 (1) (2013) 4349.
11. Raghavan S., Small H., Lowalekar V., *Handbook for Cleaning/Decontamination of Surfaces*, (2007) 459-483.
12. Bishopp J., *Handbook of Adhesives and Sealants*. (2005) 163-214.
13. Salghi R., Bazzi L., Hammouti B., Kertit S., *Bull. Electrochem.* 16 (2000) 272.
14. El Issami S., Bazzi L., Mihit M., Hammouti B., Kertit S., Ait Addi E., Salghi R., *Pig.Res.Tech.* 36 (2007)161.
15. Larabi L., Harek Y., Benali O., Ghalem S., *Prog. Org. Coat.* 54 (2005) 256.
16. Larabi L., Benali O., Mekelleche S. M., Harek Y., *Appl. Surf. Sci.* 253(2006)1371.
17. Barouni K., Bazzi L., Salghi R., Mihit M., Hammouti B., Albourine A., El Issami S., *Mater.Lett.*, 62 (2008) 3325.
18. Mihit M., Salghi R., El Issami S., Bazzi L., Hammouti B., Ait Addi E., Kertit S., *Pig. Res.Tech.* 35(2006)151.
19. El Issami S., Bazzi L., Mihit M., Hilali M., Salghi R., Ait Addi E., *J. Phys. IV.* 123 (2005) 307.



20. Zarrouk A., Zarrok H., Salghi R., Hammouti B., Bentiss F., Touir R., Bouachrine M., *J. Mater. Environ. Sci.* 4 (2013)177.
21. Anejjar A., Salghi R., Zarrouk A., Benali O., Zarrok H., Hammouti B., Al-Deyab S.S., Benchat N., Elaattiaoui A., *Int. J. Electrochem. Sci.* 8 (2013)11512.
22. Ben Hmamou D., Salghi R., Zarrouk A., Zarrok H., Hammouti B., Al-Deyab S.S., Bouachrine M., Chakir A., Zougagh M., *Int. J. Electrochem. Sci.* 7(2012) 5716.
23. Mihit M., Laarej K., Abou El Makarim H., Bazzi L., Salghi R., Hammouti B., *Arab. J. Chem.* 3 (2010) 55.
24. Refaey S. A. M., Taha F., El-Malak A. M. A., *Int. J. Electrochem. Sci.* 1 (2006) 80.
25. Kaniskan N., Ogretir C., *J. Mol. Struct. (Theochem)*, 45 (2002) 584.
26. Benali O., Larabi L., Mekelleche S.M., Harek Y., *J. Mater. Sci.* 41(2006) 7064.
27. Vracar L-M., Drazic D.M., *Corros. Sci.* 44 (2002)1669.
28. McCafferty E., *Corrosion Control by Coating*, in: H. Leidheiser (Ed.), Science Press, Princeton, JJ, (1979) 279.
29. Anejjar A., Salghi R., Zarrouk A., Benali O., Zarrok H., Hammouti B., Ebenso E.E., *J. Assoc. Arab Univers. Bas. Appl. Sci.* 15 (1) (2014) 21.
30. Mihit M., Bazzi L., Salghi R., Hammouti B., El Issami S., Ait Addi E., *Int. Sci. J. Altern. Ener. Ecol.* 62 (2008) 173.
31. Anejjar A., Zarrouk A., Salghi R., Ben Hmamou D., Zarrok H., Al-Deyab S. S., Bouachrine M., Hammouti B., Benchat N., *Int. J. Electrochem. Sci.* 8 (4) (2013) 5961.
32. Anejjar A., Zarrouk A., Salghi R., Zarrok H., Ben Hmamou D., Hammouti B., Elmahi B., Al-Deyab S.S., *J. Mater. Environ. Sci.* 4 (5) (2013)583.
33. Senhaji B., Ben Hmamou D., Salghi R., Zarrouk A., Chebli B., Zarrok H., Hammouti B., AlDeyab S. S., *Int. J. Electrochem. Sci.* 8 (2013) 6033.
34. Bammou L., Salghi R., Zarrouk A., Zarrok H., Al-Deyab S. S., Hammouti B., Zougagh M., Errami M., *Int. J. Electrochem. Sci.* 7 (9) (2012) 8974.
35. Belkhaouda M., Bammou L., Salghi R., Zarrouk A., Ben Hmamou D., Zarrok H., Assouag M., Hammouti B., Al-Deyab S. S., *Der Pharma. Lett.* 5 (2) (2013) 143.
36. Belkhaouda M., Bammou L., Zarrouk A., Salghi R., Ebenso E. E., Zarrok H., Hammouti B., Bazzi L., Warad I., *Int. J. Electrochem. Sci.* 8 (5) (2013) 7425.
37. Belkhaouda M., Bammou L., Salghi R., Zarrouk A., Ebenso E. E., Zarrok H., Hammouti, *Int. J. Electrochem. Sci.* 8 (9) (2013) 10987.
38. Ben Hmamou D., Zarrouk A., Salghi R., Zarrok H., Ebenso E. E., Hammouti B., Kabanda M.M., Benchat N., Benali O., *Int. J. Electrochem. Sci.* 9 (1) (2014)120.
39. Afia L., Salghi R., Bammou L., Bazzi El., Hammouti B., Bazzi L., Bouyanzer A., *J. Saudi Chem. Soc.* 18 (1) (2014) 16.
40. Salghi R., Anejjar A., Benali O., Al-Deyab S. S., Zarrouk A., Errami M., Hammouti B., Benchat N., *Int. J. Electrochem. Sci.* 9 (6) (2014) 3087.
41. El Mouden O., Anejjar A., Messali M., Salghi R., Ali Isma H., Hammouti B., *Chem Sci Rev Lett.* 3(11) (2014) 579.
42. Tsuru T., Haruyama S., Gijutsu B., *J. Jpn. Soc. Corros. Eng.* 27 (1978) 573.
43. Rinki G., Siddiqi W. A., Bahar A., Hussan. J., *E-Journal Chem.* 7(S1) (2010) S319.
44. Martinez S., Stern I., *Appl. Surf. Sci.* 199 (2002) 83.
45. Guan N.M., Xueming L., Fei L., *Mater. Chem. Phys.* 86 (2004) 59.
46. Yurt A., Balaban A., Kandemir S. U., Bereket G., Erk B., *Mater.Chem.Phys.* (85) (2004) 420.
47. Langmuir I., *J. Am. Chem. Soc.* 39 (1947) 1848.
48. Mishra V., Saxena D.K., *Synth. React. Inorg. Met. Org. Chem.* 17 (1987) 987.
49. Devanathan M.A.V., Stachurski Z., *Proc. R. Soc. (Lond.)*, A 270 (1962) 90.
50. Abiola O.K., Oforka N.C., *Mater. Chem. Phys.* 83 (2004) 315.
51. Li X., Deng S., Fu H., Li T., *Electrochim. Acta.* 54 (2009) 4089.

(2015); <http://www.jmaterenvirosnci.com/>